



## Design and characterization of a novel amphiphilic chitosan nanocapsule-based thermo-gelling biogel with sustained *in vivo* release of the hydrophilic anti-epilepsy drug ethosuximide

Meng-Hsuan Hsiao <sup>a,1</sup>, Mikael Larsson <sup>a,b,1</sup>, Anette Larsson <sup>b</sup>, Hanne Evenbratt <sup>b</sup>, Ying-Yu Chen <sup>c</sup>, You-Yin Chen <sup>d</sup>, Dean-Mo Liu <sup>a,\*</sup>

<sup>a</sup> Department of Materials Science and Engineering, National Chiao Tung University, 1001 Ta-Hseuh Road, Hsinchu City, 300 Taiwan, ROC

<sup>b</sup> Department of Chemical and Biological Engineering, Chalmers University of Technology, Gothenburg, 41296, Sweden

<sup>c</sup> Department of Material Engineering, University of Southern California, 1204 w 24th st. LA CA 90007, USA

<sup>d</sup> Department of Biomedical Engineering, National Yang Ming University, No.155, Sec.2, Linong Street, Taipei, 112 Taiwan, ROC

### ARTICLE INFO

#### Article history:

Received 27 February 2012

Accepted 20 May 2012

Available online 28 May 2012

#### Keywords:

Amphiphilic chitosan

Drug delivery

Nano capsules

Thermo responsive

*In vivo*

### ABSTRACT

Thermo-gelling injectable nanogels, with no burst release of loaded drug, were prepared by a simple route by combining self assembled nanocapsules of amphiphilically modified chitosan with glycerophosphate di-sodium salt and glycerol. The potential as a depot drug delivery system was demonstrated *in vivo* through the therapeutic effect of ethosuximide (ESM) loaded nanogels, suppressing spike wave discharges (SWDs) in Long Evan rat model. Simultaneously clearance of gels from the site of administration was monitored non-invasively using MRI. The gel structure was characterized using TEM and SEM, confirming the gels to be an assembly of nanocapsules and using two-photon microscopy to visualize the network structure. *In vitro* drug release studies using ESM revealed that the nanogels exhibited extended, mostly Fickian release. Finally, all investigated formulations displayed excellent cytotoxicity data determined by MTT assay using human retinal pigmented epithelium cells. All presented properties are highly desirable for injectable depot gels for drug delivery.

© 2012 Elsevier B.V. All rights reserved.

### 1. Introduction

In this study we set out to prepare chitosan based injectable drug loaded hydrogels without burst release, where a gel-network and drug encapsulation could be achieved using a single modified chitosan component, enabling extremely simple preparation procedure. This is of relevance as thermo-gelling formulations can be easily administrated to provide sustained systemic or local therapeutic effect when loaded with drugs or [1–4], but with burst release of a fraction of loaded drug being a commonly observed problem [5]. In addition, drug release of small hydrophilic molecules is often completed in less than 24 h [6]. The concept of solving this problem by encapsulating the drug into carriers subsequently embedded in the thermo-gelling matrix has been successful demonstrated previously [4,6,7]. However, to the authors' knowledge all previous studies involve different components and preparation steps for the drug loading into nanocarriers and preparation of the thermo-gelling solution, respectively.

When designing an injectable medical hydrogel the following requirements need considered and met for an ideal performance

of the formulation, as stated by [8]: (1) a sol-to-gel transition before and after injection into the sites of injury, (2) a biodegradable or gradually dissolving character, (3) both the hydrogel and the degradation products should be biocompatible, and (4) the gel should present desirable properties for the intended application, for instance, sustained release profile for drug delivery systems, or cell adhesive capabilities for tissue engineering.

Chitosan (CS) is a polysaccharide which has been widely studied for use in biomedical applications as it presents desirable properties such as: biocompatibility, biodegradation, bioadhesivity, anti-bacterial effects and no toxicity [9–12].

One common and straight forward approach to achieve CS solutions with thermo-induced gelling is to include polyol salts such as; disodium-, ammonium hydrogen-, glycerol-, sorbitol-, fructose- or glucose-phosphate salts. These transform purely pH-dependent chitosan solutions into temperature-controlled pH-dependent chitosan solutions [2,13–17]. Such solutions are typically liquids at low temperatures, but form gels at elevated temperatures, making them suitable as injectable *in vivo* gelling systems.

Recently, chitosan based nanoscale drug-carriers formed from a new type of amphiphilic chitosan, namely carboxymethyl-hexanoyl chitosan (CHC) was successfully synthesized in this lab. Native chitosan was modified by partial substitution with hydrophilic

\* Corresponding author. Tel.: +886 3 571 2121x55391; fax: +886 3 572 4272.

E-mail address: [deanmo\\_liu@yahoo.ca](mailto:deanmo_liu@yahoo.ca) (D.-M. Liu).

<sup>1</sup> Both authors contributed equally to this work.

carboxymethyl groups to increase the solubility of the chitosan polysaccharide chain in water and by partial substitution with hydrophobic hexanoyl groups to increase the amphiphilic character [18]. The CHC demonstrated self-assembly into nanocapsules about 200 nm in size in aqueous environment, and the capsules demonstrated good drug loading properties [18–20]. In a previous study, we demonstrated extremely slow release of hydrophobic drug from such CHC nanocarriers embedded in a macroscopic calcium alginate gel [21]. Based on those earlier findings and the previously mentioned reports on preparation of thermo-gelling chitosan solutions using polyol salts, it was investigated if CHC could be used both to encapsulate drug, minimizing burst release, and to form a thermo-gelling network in the presence of a polyol salt. Such a formulation would allow for extremely easy sample preparation and because of the previously reported low cytotoxicity and host irritation of CHC it would hold great potential as an injectable drug depot platform [21,22].

Indeed, when CHC nanocapsules in water were mixed with glycerol and sodium  $\beta$ -glycerophosphate ( $\beta$ -GP) thermo-gelling solutions were formed. The formed CHC hydrogels were characterized with regard to; gelation time, rheological properties and structure using two-photon microscopy (TPM), SEM and TEM. The *in vitro* drug release from the formed gels was investigated using the highly water-soluble drug Ethosuximide (ESM). Cell cytotoxicity was investigated using a MTT assay. Finally, the feasibility of the CHC hydrogels as an injectable depot drug delivery system was demonstrated through the successful suppression of spike wave discharges (SWDs) in rats, combined with *in vivo* magnetic resonance imaging (MRI) of hydrogel clearance from the site of injection.

## 2. Methods

### 2.1. Materials

Carboxymethyl hexanoyl Chitosan (CHC), M.W. = 150,000 g/mol and viscosity = 2500–3500 cP (4% solution), was bought from Advanced Delivery Technology Inc., Hsinchu, Taiwan under the name AC-SAC (nanocarrier), and its chemical identity was confirmed to be similar to previously reported CHC [18] using NMR (supplementary material Fig. S1). Glycerol, Ethosuximide (ESM), Pyrene and chemicals to prepare simulated body fluid (SBF); NaCl, NaHCO<sub>3</sub>, KCl, K<sub>2</sub>HPO<sub>4</sub>, MgCl<sub>2</sub>, HCl, CaCl<sub>2</sub>, Na<sub>2</sub>SO<sub>4</sub>, and (CH<sub>2</sub>OH)<sub>3</sub>CNH<sub>2</sub> were bought from Sigma-Aldrich.  $\beta$ -glycerol phosphate disodium salt hydrate ( $\beta$ -GP) was bought from Merck. Genipin was purchased from Challenge Bioproducts Co., Taiwan.

### 2.2. Preparation of CHC thermo-gelling solutions

Solutions with thermally induced sol–gel transition were prepared as follows: 1–3 g (x) of CHC powder was dissolved in 100 ml distilled water (DW), the solution was then cooled in an ice bath. Subsequently, 0.5, 1 or 1.5 g (y)  $\beta$ -GP was dissolved in 9 ml of the CHC solution under stirring on ice. After mixing, 0–1 ml (z) glycerol + DW (total volume 1 ml) was dropped into 9 ml of the CHC/ $\beta$ -GP solution in ice bath to prepare 10 ml CHC- $\beta$ -GP-glycerol hybrid solution. The samples were named accordingly Cx- $\beta$ y-Gz. See supplementary material Table S1 for amounts used and sample naming.

### 2.3. Gelation time and rheological analysis

The time required at 37 °C to form a gel (designated as gelation time) was determined using a vial tilting method, where no flow within 1 minute of inverting the vial was the criterion for gel state [23,24]

Rheological properties of samples were monitored when pre-gelling solution was moved from 4 to 37 °C using an ARES rheometer

(Rheometric Scientific, Piscataway, NJ) fitted with a cone-plate tool, at a frequency of 10 rad/s and a strain of 1%. The diameter of the plate was 25 mm. The force and displacement were recorded, and the dynamic storage ( $G'$ ) and loss modulus ( $G''$ ) were determined as functions of time.

### 2.4. Morphological characterization of CHC nanogels

Morphological evaluation of formed and subsequently dried or freeze-dried CHC gels was performed by transmission electron microscopy (TEM) and scanning electron microscopy (SEM), respectively. The phase distribution in wet nanogels was analysed using two-photon microscopy (TPM) analysis of gel formed from CHC nanocarriers that were loaded with pyrene ( $10^{-4}$  M) as previously described [20]. The structure of eroded gel fragments was determined by SEM analysis of nanogel fragments released after submersion in DW for one day (see supplementary material for details).

### 2.5. *In vitro* drug release

*In vitro* release studies in SBF were conducted on nanogels loaded with 0.1 g of the antiepileptic drug ethosuximide (ESM), crosslinked with genipin (100 ppm) [25] to eliminate the effect of gel disintegration (see supplementary material for details).

### 2.6. *In vivo* studies

*In vivo* therapeutic effect of ESM released from implanted CHC nanogels was evaluated as follows. ESM loaded nanogels were subcutaneously injected into five Long Evan rats (300 g, National Laboratory Animal Centre, Taiwan) which spontaneously present spike-wave discharges (SWDs) [26,27]. The SWDs of Long Evan rats have been suggested to be an absence like seizure activity that is known to be suppressed by the antiepileptic drug ESM [26,28,29]. An electrophysiological method to record spike-wave discharges (SWDs) was used to evaluate the therapeutic effects of ESM released from the implanted CHC nanogels. Furthermore, magnetic resonance imaging (MRI) was noninvasively performed to investigate the clearance, of implanted CHC nanogels *in vivo*. Animal experiments and treatment of test animals were performed according to institutional ethical guidelines. Approval for the animal experiments was obtained from the Animal Research Committee of National Chiao-Tung University and National Taiwan University (see supplementary material for details).

### 2.7. Cell culture cytotoxicity

Different formulations of nanogels were investigated with regard to cytotoxicity by an MTT cell proliferation assay using ARPE-19 cells (see supplementary material for details).

### 2.8. Statistical analysis

For evaluation of *in vivo* therapeutic effect repeated measures analysis of variance (ANOVA) was used. Differences with  $p$  values of less than 0.05 were considered statistically significant. All statistical analyses were performed using SPSS (Statistical Package for the Social Sciences, version 10.0; SPSS, Chicago, IL, USA) for Windows. Other data are when applicable reported as mean  $\pm$  SD, with number of replicates indicated.

## 3. Results

### 3.1. Gelation of the CHC hydrogels

CHC self-assembles into nanocapsules in aqueous environment. At acidic to neutral pH the nanocapsules carry positive charges on their

shell, derived from the protonation of amino groups. Here  $\beta$ -GP was used to neutralize the positive charge and reduce repulsive force between CHC nanocapsules at elevated temperatures, giving rise to a sol–gel transition with increased temperature. Furthermore, glycerol was added to provide increased gel strength, based on our previous experiences. Fig. 1a shows the concept of CHC nanogel preparation.

The CHC pre-gelling solution is virtually a viscous liquid at low temperature, i.e. 4–10 °C, which exhibits flow under its own weight. However, the solution formed a gel within reasonable time when exposed to 37 °C or above, as demonstrated in Fig. 1b.

The gelation time of different formulations when pre-gelling solution was moved from 4 to 37 °C was determined using the vial tilting method, see supplementary material Table S1. It was found that  $\beta$ -GP was a prerequisite for thermally induced gelling. Furthermore, a considerable reduction in the gelation time was observed for all formulations with increasing CHC content. The gelation time also decreased with increased addition of both  $\beta$ -GP and glycerol. No gelation was observed after 24 h for the samples with the lowest CHC content and no glycerol, irrespectively of  $\beta$ -GP content. The longest observed gelation times were > 1 h, while the shortest observed gelation time was about 150 s for the sample with the highest investigated CHC,  $\beta$ -GP and glycerol contents (C3- $\beta$ 15-G10).

Rheological analysis revealed that initially the loss modulus  $G''$  was larger than the storage modulus  $G'$ , often taken as a criterion for a liquid. However, during the thermally induced gelation  $G'$  increased more rapidly than  $G''$ , so that a crossover point was observed (supplementary material Fig. S3). Such a crossover is often taken as a sign of gelation and the observed crossover-times were in

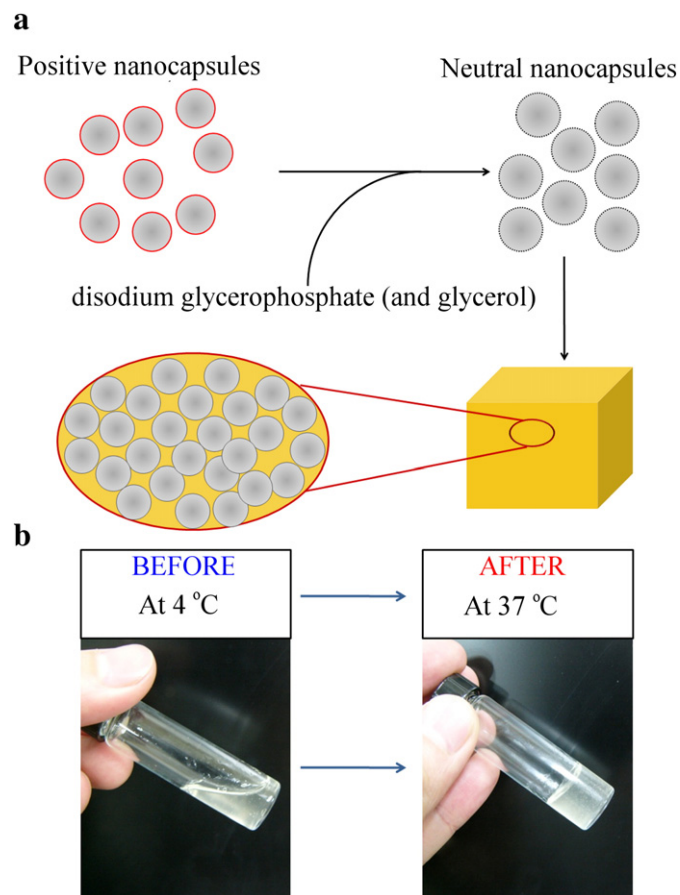


**Fig. 1.** The concept of CHC nanogel preparation and thermo-gelling. (a) Positively charged nanocapsules were neutralized by glycerophosphate di-sodium salt, glycerol was added to improve the hardness of formed CHC nanogels. (b) CHC solution (C2- $\beta$ 5-G10) before and after thermally induced gelation.

reasonable agreement with the gelation times determined using the vial tilting method.

### 3.2. Structure of the CHC hydrogels

TEM analysis of dried gel revealed that the nanogel was composed of numerous nanocapsules Fig. 2a. The diameters observed in TEM was about 50–200 nm, which is similar to previous observations [19].

SEM analysis of freeze dried gel samples revealed structures interpreted as capsules having sizes ranging from about 100 nm to 500 nm (Fig. 2b). The fact that the observed sizes are larger than those observed using TEM is most likely due to swelling of the particles in solution. It is important to point out that CHC is in fact a minority component in the gels, the theoretical concentration per dry mass of the freeze dried samples ranged from about 35% to 14% and the CHC concentration per volume would be as low as about 2%. Thus major part of the samples would not be nanocapsules even if all CHC was present in that form. Furthermore, there is the possibility that some CHC existed as free polymer chains rather than capsules and there was a big risk that any capsule structures present would be destroyed during the freeze drying process. Any material other than nanocapsules present in the samples would make the detection of nanocapsules difficult due to them being covered by the layer-like structures formed during freeze-drying. The fact that nanocapsules could be observed after freeze-drying, despite the complicating factors discussed above, clearly indicates the presence of nanocapsules in the formed gels. From the TEM and SEM results it is concluded that CHC did exist as nanocapsules in the formed gels.

To get an indication on the structure of the formed network, nanogel loaded with the hydrophobic fluorescent substance pyrene was analysed using TPM. Pyrene would mainly be located in the hydrophobic domains of CHC, thus the acquired images reflects the formed CHC network. The TPM-analysis revealed that the nanogel was composed of a continuous network, with phase domains having sizes in the micrometer range (Fig. 2c).

It was observed that the nanogels disintegrated upon submersion in DW or SBF (Supplementary material Fig. S4). SEM analysis of fragments released from the bulk CHC gel during submersion in DW revealed that the gels disintegrated through the released of particles having sizes of several hundreds of nanometres (Fig. 2d), where the released particles were composed of an assembly of smaller objects.

### 3.3. In vitro drug release

Given the observation that the CHC nanogels disintegrated into nano-sized fragments in release media, a small amount of genipin was added to crosslink and thus stabilize the nanogels prior to *in vitro* release studies, this to eliminate any influence from gel erosion (disintegration) on the release profiles and release kinetics. The addition of genipin did not significantly influence the initial (1–2) days release from the gels (supplementary material Fig. S4). CHC nanogels loaded with 10 mg/ml of the hydrophilic antiepileptic drug ethosuximide (ESM) were prepared using different amounts of  $\beta$ -GP and glycerol in the pre-gelling solutions. As seen in Fig. 3, gels prepared without glycerol and with low amounts of  $\beta$ -GP displayed a rapid release of the loaded drug with 50% of the drug being released in about 2 days. Increasing  $\beta$ -GP or glycerol content lead to a slower release, with only about 20% of the loaded drug being released after 20 days for the formulation C3- $\beta$ 15-G0. Of importance is that none of the formulations displayed burst release. To get an indication of the mechanism of the drug release, the cumulative release up to about 60%, as suggested by others [30,31], was fitted to the equation:

$$\frac{M_t}{M_\infty} = kt^n \quad (1)$$

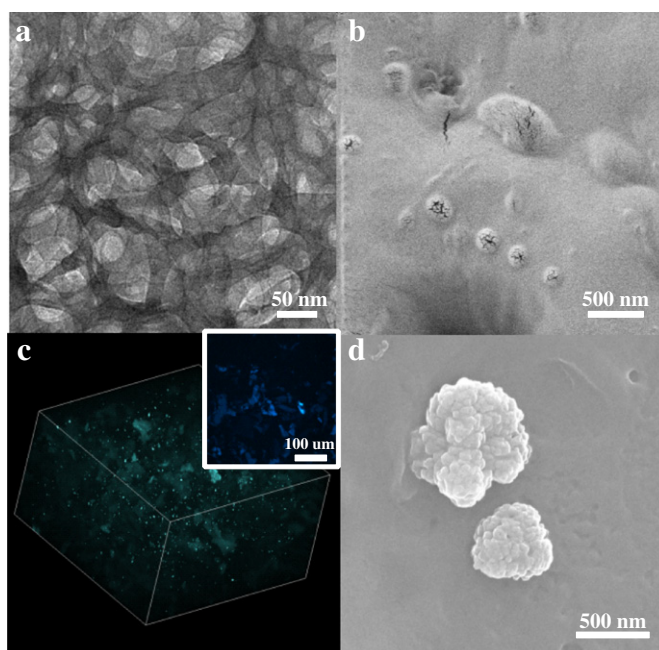


**Fig. 2.** Microscopy images of CHC gels. (a) TEM image of CHC nanogel (C3-β5-G10) dried after gelation. (b) SEM image showing CHC nanogel (C3-β5-G5) after freeze-drying. (c) Two-photon microscopy image of pyrene loaded CHC nanogel network (C3-β5-G5) dimensions are  $424 \times 424 \times 255 \mu\text{m}$ , insert is 1-D image. (d) SEM images of gel fragments released from submerged nanogel (C3-β5-G10).

where  $M_t$  is the amount of drug released at time  $t$ ,  $M_\infty$  is the amount of drug released at infinite time,  $k$  and  $n$  are both constants. The value of  $n$  is commonly taken as an indication of the release mechanism, where a value of 0.5 for slabs, or 0.43 for spheres suggests diffusion controlled (Fickian) release, while a value of 1 for slabs or 0.85 for spheres suggests relaxation controlled release. Values in between indicates an anomalous release mechanism [30,31]. The fit of Eq. (1) to release data suggests that the *in vitro* release was rather well described by Fickian release mechanism (see Table 1 and fit to data in Fig. 3).

#### 3.4. *In vivo* therapeutic effect and nanogel clearance

To evaluate the *in vivo* performance of drug loaded nanogels, Long Evan rats, which spontaneously present SWDs [26,27], were used as test subjects. The SWDs of Long Evan rats have been suggested to be an absence like seizure activity that is known to be suppressed by the

antiepileptic drug ESM [26,28,29]. Thus, the therapeutic effect of ESM loaded nanogels in the chosen model was expected to give good initial indications on the feasibility of the nanogels for future drug delivery therapy. The rats received a 1 ml subcutaneous implant of the nanogel C3-β5-G5, containing 10 mg/ml ESM, and gelation at the site of administration was confirmed using MRI. The ESM treatment reduced the number of recorded SWDs to about 50% on days 1–3 after injection. From day 4 the number of SWDs increased, reaching pre-treatment levels at days 6–7. In addition, the amplitude of the SWDs that did occur during days 2–3 was much less than that observed prior to treatment and during days at which the number of SWDs was not significantly reduced. MRI analysis revealed that the nanogel clearance was completed during a time period similar to the duration of the therapeutic effect. The clearance initially proceeded at a relatively low rate up to day 2, between days 2 – 5 it accelerated, leading to about 20% of the gel remaining at day 5. At day 7, the implanted nanogel was all but gone (Fig. 4).

#### 3.5. Cytotoxicity of CHC nanogels

Since the CHC nanogels were mainly composed of water and chitosan, they were likely to be highly biocompatible, as reported for native thermo-gelling chitosan gels [32]. The cytotoxicity of different formulations of CHC nanogels was investigated by the MTT assay using Human retinal pigmented epithelium cells (ARPE-19). As seen in Fig. 5, only a

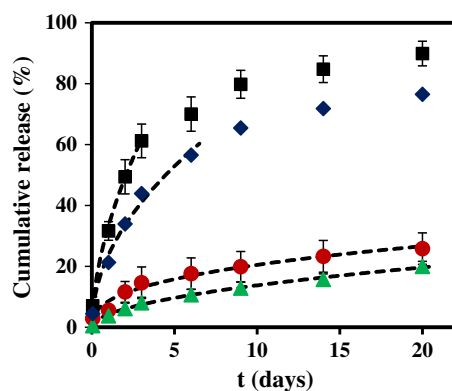


**Fig. 3.** Cumulative drug release for (a) Different formulations loaded with ESM; C3-β5-G0 (■), C3-β5-G5 (◆), C3-β5-G10 (●) and C3-β15-G0 (▲) Error bars indicate one standard deviation ( $n = 3$ ). Dashed lines are fit of Eq. (1) to data with exponents ( $n$ ) as seen in Table 1.

**Table 1**  
The  $n$  and  $R^2$  values for formulations used for *in vitro* release experiments, from fit of data to Eq. (1).

| Sample        | $n$  | $R^2$ |
|---------------|------|-------|
| ESM-C3-β5-G0  | 0.56 | 1.0   |
| ESM-C3-β5-G5  | 0.50 | 0.99  |
| ESM-C3-β5-G10 | 0.38 | 0.98  |
| ESM-C3-β15-G0 | 0.51 | 1.0   |

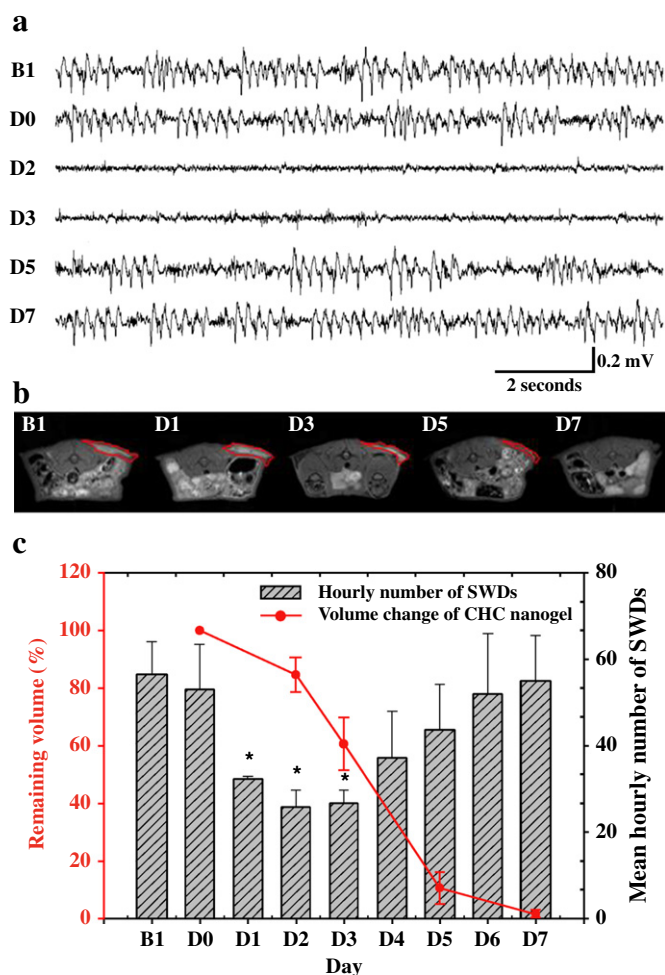


**Fig. 4.** Therapeutic effect and *in vivo* disintegration of ESM loaded, subcutaneously implanted CHC nanogels. (a) Typical SWDs recorded one day before injection (B1), immediately after injection (D0), and 2–7 days after injection (D2–D7). (b) MR images of the implanted CHC nanogel at different times. (c) Hourly number of SWDs and remaining gel volume before and at given times after injection. Data presented as mean, error bars indicate one standard deviation ( $n = 5$ ).

very small decrease in cell viability could be detected for the nanogels with the highest  $\beta$ -GP and glycerol contents (C3- $\beta$ 15-G0 and C3- $\beta$ 5-G10), for all other investigated samples there was no significant difference in cell viability compared to the control.

#### 4. Discussion

A novel injectable thermo-gelling nanogel with no burst release was developed based on combination of nanocapsules of CHC,  $\beta$ -GP and glycerol.

Different formulations were investigated with regard to gelation time when transferred from 4 °C to 37 °C. The results presented in Table S1 revealed that the gelation time was strongly dependent on composition of the pre-gelling solution. In particular,  $\beta$ -GP was a prerequisite for thermo induced gelation and the gelation time was dramatically decreased with increasing CHC content. This reduction in gelation time is surely a result of more CHC macromolecules or preferably, nanocapsules aggregating or coagulating, reaching a continuous network in a shorter time under the same chemical environment. The formed gels had a phase separated structure with micrometer sized CHC containing regions forming a continuous network, as seen from two photon microscopy analysis of pyrene loaded nanocapsules

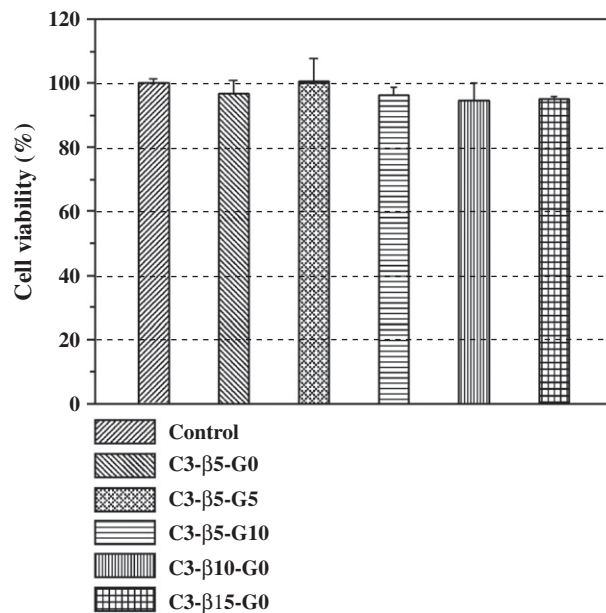


**Fig. 5.** Cell Viability of ARPE-19 cells cultured in media containing various formulations of CHC nanogels. Error bars indicate one standard deviation ( $n = 3$ ).

(Fig. 2c). Furthermore, the observations revealed that gelation is largely promoted not only by  $\beta$ -GP, as reported previously for native chitosan [32,33], but also by the presence of glycerol. Rheological analysis revealed that CHC solutions containing glycerol formed harder gels than those prepared using only  $\beta$ -GP (supplementary material Fig. S3). The rheological analysis also revealed that the storage modulus of the reported gels evolved similarly to previous reported chitosan based thermogelling systems [6,14,16], forming relatively weak gels in comparison to systems based on synthetic thermogelling polymers [7,15] or *in situ* gelling systems that utilizes mechanisms other than thermogelation [15,21].

The used CHC is known to exist as self-assembled nanocapsules in solution [19,20]. TEM analysis of prepared and subsequently dried gels as well as SEM analysis of freeze-dried gels revealed that nanocapsules were also present in the formed gels, as seen in Fig. 2a, b. Thus, the network in the nanogels was probably composed of nanocapsules connected through physical interactions, e.g., hydrophobic interactions and hydrogen bonds. As such, the CHC nanogels likely had a network structure significantly different from conventional chitosan-based hydrogels reported in literature where the continuous network is composed of polymer chains. The non-covalent nature of the network should allow for time dependent disintegration of the hydrogels, which would be desirable for transient implant applications. Indeed, after long-term incubation in SBF or DW, the bulk CHC gels were found to swell and slowly disintegrate (Supplementary material Fig. S4). As seen from SEM analysis of released gel fragments (Fig. 2d), the gels mainly disintegrated through the release of nano-sized fragments, in turn composed of an assembly of smaller objects, likely CHC nanocapsule assemblies. Given the simple disintegration route, it seemed probable that the gels could also disintegrate *in vivo*, and that the resulting nanoparticles and primary nanocapsules could be efficiently transported away from the remaining bulk gel.

The fact that the CHC nanogels were composed of self-assembled CHC nanocapsules, which have been shown to efficiently encapsulate drugs and have extended release profiles [19,20], surely suggests that the gels could be exceptionally suitable for depot drug delivery applications in which a sustained release with minimal burst release is desired. *In vitro* release studies revealed that in accordance with the aim of this study no burst release was observed for any of the

formulations (Fig. 3). The fitting of Eq. (1) to data suggests, guided by previous works [30,31], that the *in vitro* drug release from the gels was rather diffusion controlled. It needs to be emphasized that the lack of burst release and in some cases very slow release strongly indicates that the drug was indeed encapsulated in the nanocapsules, and that diffusion out of those are the rate limiting step. The differences in release rates between the formulations were probably due to different network structures in the gels and differences in the chemical environment in the gels. The exact reason would be interesting to investigate further, but is beyond the scope of this study.

Based on the release data and analysis the nanogels have potential for long term sustained release, such as drug depot formulations. The therapeutic effect of ESM was demonstrated *in vivo* utilizing Long Evans Rats as the animal model, and was found to coincide with the *in vivo* clearance of the hydrogels from the site of administration (Fig. 4). Apparently therapeutic drug levels were not reached until day 1, and remained until day 4, in contrast, for free ESM there is a rapid initial response 1 h after administration [34] and the effect is significantly lower already after 24 h. From the *in vivo* release study it can be concluded that the nanogels seem promising as a depot sustained release platform. However, further animal studies will be needed to investigate the *in vivo* performance of different nanogel compositions, using different drugs.

Given the promising *in vivo* results, the cytotoxicity of the nanogels was evaluated using Human retinal pigmented epithelium cells. The results revealed that the all investigated nanogel formulations exhibited very low cytotoxicity (Fig. 5), further strengthening the potential of said nanogels in biomedical applications.

## 5. Conclusion

In summary, the presented nanogels display excellent properties with regard to usage as an injectable depot drug delivery system. The preparation procedure is very easy as CHC both encapsulate the drug, with reduced burst release and release rate as consequences, and is the gel network forming constituent. The gels display sol–gel transition when exposed to physiological temperature, excellent cytotoxicity data and successful usage as a depot drug delivery system *in vivo*. The gels presented in this proof of concept study displays many interesting properties that could be investigated in detail. In particular, future studies would be to develop the characterization of the *in vivo* performance using different gel formulations, animal models and drugs and to investigate the use of the nanogels in cancer therapy or other indications. On a more fundamental level it would be interesting to characterize the gel network formation during the gelation and to investigate how structure and composition influences properties such as *in vitro* drug release, mechanical properties and *in vivo* disintegration of the gels.

## Acknowledgements

Thanks to Dr. C.-H. Hsieh and Dr. J.-H. Chen (7T animal MRI Core Lab of the Neurobiology and Cognitive Science Center) for technical and facility support and MRI experiments performed at National Taiwan University. We further, acknowledge the Centre for Cellular Imaging at the University of Gothenburg for the use of imaging equipment and for the support from the staff. This study was supported by the National Science Council, Taiwan, Republic of China, under the project contract NSC 99-2113-M-009-013-MY2-3060. The work was performed in collaboration with the VINN Excellence Centre SuMo Biomaterials (Supermolecular Biomaterials – Structure dynamics and properties) and the associated research school BIOSUM.

## Appendix A. Supplementary data

Supplementary data to this article can be found online at <http://dx.doi.org/10.1016/j.jconrel.2012.05.038>.

## References

- [1] H.T. Ta, C.R. Dass, D.E. Dunstan, Injectable chitosan hydrogels for localised cancer therapy, *J. Control. Release* 126 (2008) 205–216.
- [2] X. Li, X. Kong, J. Zhang, Y. Wang, Y. Wang, S. Shi, G. Guo, F. Luo, X. Zhao, Y. Wei, Z. Qian, A novel composite hydrogel based on chitosan and inorganic phosphate for local drug delivery of camptothecin nanocolloids, *J. Pharm. Sci.* 100 (2011) 232–241.
- [3] J.F. Mano, Stimuli-responsive polymeric systems for biomedical applications, *Adv. Eng. Mater.* 10 (2008) 515–527.
- [4] E. Ruel-Gariépy, J.-C. Leroux, In situ-forming hydrogels—review of temperature-sensitive systems, *Eur. J. Pharm. Biopharm.* 58 (2004) 409–426.
- [5] A. Hatefi, B. Amsden, Biodegradable injectable in situ forming drug delivery systems, *J. Control. Release* 80 (2002) 9–28.
- [6] E. Ruel-Gariépy, G. Leclair, P. Hildgen, A. Gupta, J.C. Leroux, Thermosensitive chitosan-based hydrogel containing liposomes for the delivery of hydrophilic molecules, *J. Control. Release* 82 (2002) 373–383.
- [7] X.-Z. Zhang, P. Jo Lewis, C.-C. Chu, Fabrication and characterization of a smart drug delivery system: microsphere in hydrogel, *Biomaterials* 26 (2005) 3299–3309.
- [8] L. Yu, J. Ding, Injectable hydrogels as unique biomedical materials, *Chem. Soc. Rev.* 37 (2008) 1473–1481.
- [9] M. Dash, F. Chiellini, R.M. Ottenbrite, E. Chiellini, Chitosan—a versatile semi-synthetic polymer in biomedical applications, *Prog. Polym. Sci.* 36 (2011) 981–1014.
- [10] E. Khor, L.Y. Lim, Implantable applications of chitin and chitosan, *Biomaterials* 24 (2003) 2339–2349.
- [11] V. Dodane, V.D. Vilivalam, Pharmaceutical applications of chitosan, *Pharm. Sci. Technol. Today* 1 (1998) 246–253.
- [12] M. Prabakaran, J.F. Mano, Chitosan-based particles as controlled drug delivery systems, *Drug Deliv.* 12 (2004) 41–57.
- [13] D. Filion, M. Lavertu, M.D. Buschmann, Ionization and solubility of chitosan solutions related to thermosensitive chitosan/glycerol-phosphate systems, *Biomacromolecules* 8 (2007) 3224–3234.
- [14] A. Chenite, M. Buschmann, D. Wang, C. Chaput, N. Kandani, Rheological characterisation of thermogelling chitosan/glycerol-phosphate solutions, *Carbohydr. Polym.* 46 (2001) 39–47.
- [15] H.J. Chung, T.G. Park, Self-assembled and nanostructured hydrogels for drug delivery and tissue engineering, *Nano Today* 4 (2009) 429–437.
- [16] X. Li, X. Kong, X. Wang, S. Shi, G. Guo, F. Luo, X. Zhao, Y. Wei, Z. Qian, Gel–sol–gel thermo-gelation behavior study of chitosan–inorganic phosphate solutions, *Eur. J. Pharm. Biopharm.* 75 (2010) 388–392.
- [17] L.S. Nair, T. Starnes, J.-W.K. Ko, C.T. Laurencin, Development of injectable thermogelling chitosan–inorganic phosphate solutions for biomedical applications, *Biomacromolecules* 8 (2007) 3779–3785.
- [18] T.-Y. Liu, S.-Y. Chen, Y.-L. Lin, D.-M. Liu, Synthesis and characterization of amphiphatic carboxymethyl-hexanoyl chitosan hydrogel: water-retention ability and drug encapsulation, *Langmuir* 22 (2006) 9740–9745.
- [19] K.-H. Liu, S.-Y. Chen, D.-M. Liu, T.-Y. Liu, Self-assembled hollow nanocapsule from amphiphatic carboxymethyl-hexanoyl chitosan as drug carrier, *Macromolecules* 41 (2008) 6511–6516.
- [20] K.-H. Liu, B.-R. Chen, S.-Y. Chen, D.-M. Liu, Self-assembly behavior and doxorubicin-loading capacity of acylated carboxymethyl chitosans, *J. Phys. Chem. B* 113 (2009) 11800–11807.
- [21] L.-J. Lin, M. Larsson, D.-M. Liu, A novel dual-structure, self-healable, polysaccharide based hybrid nanogel for biomedical uses, *Soft Matter* 7 (2011) 5816–5825.
- [22] T.-Y. Liu, T.-Y. Liu, S.-Y. Chen, S.-C. Chen, D.-M. Liu, Effect of hydroxyapatite nanoparticles on ibuprofen release from carboxymethyl-hexanoyl chitosan/o-hexanoyl chitosan hydrogel, *J. Nanosci. Nanotechnol.* 6 (2006) 2929–2935.
- [23] R. Jin, L.S.M. Teixeira, P.J. Dijkstra, M. Karperien, C.A. van Blitterswijk, Z.Y. Zhong, J. Feijen, Injectable chitosan-based hydrogels for cartilage tissue engineering, *Biomaterials* 30 (2009) 2544–2551.
- [24] S. Kim, S.K. Nishimoto, J.D. Bumgardner, W.O. Haggard, M.W. Gaber, Y.Z. Yang, A chitosan/beta-glycerophosphate thermo-sensitive gel for the delivery of ellagic acid for the treatment of brain cancer, *Biomaterials* 31 (2010) 4157–4166.
- [25] R.A.A. Muzzarelli, Genipin-crosslinked chitosan hydrogels as biomedical and pharmaceutical aids, *Carbohydr. Polym.* 77 (2009) 1–9.
- [26] F.Z. Shaw, S.H. Chuang, K.R. Shieh, Y.J. Wang, Depression- and anxiety-like behaviors of a rat model with absence epileptic discharges, *Neuroscience* 160 (2009) 382–393.
- [27] I. Serbanescu, M.A. Ryan, R. Shukla, M.A. Cortez, O.C. Snead, S.C. Cunnane, Lovastatin exacerbates atypical absence seizures with only minimal effects on brain sterols, *J. Lipid Res.* 45 (2004) 2038–2043.
- [28] P.-O. Polack, S. Champier, Intracellular activity of cortical and thalamic neurones during high-voltage rhythmic spike discharge in long-evans rats *in vivo*, *J. Physiol.* 571 (2006) 461–476.

- [29] F.-Z. Shaw, Is spontaneous high-voltage rhythmic spike discharge in long evans rats an absence-like seizure activity? *J. Neurophysiol.* 91 (2004) 63–77.
- [30] J. Siepman, N.A. Peppas, Modeling of drug release from delivery systems based on hydroxypropyl methylcellulose (hpmc), *Adv. Drug. Deliv. Rev.* 48 (2001) 139–157.
- [31] P.L. Ritger, N.A. Peppas, A simple equation for description of solute release ii. Fickian and anomalous release from swellable devices, *J. Control. Release* 5 (1987) 37–42.
- [32] R. Ahmadi, J.D. de Bruijn, Biocompatibility and gelation of chitosan–glycerol phosphate hydrogels, *J. Biomed. Mater. Res. A* 86A (2008) 824–832.
- [33] A. Chenite, C. Chaput, D. Wang, C. Combes, M.D. Buschmann, C.D. Hoemann, J.C. Leroux, B.L. Atkinson, F. Binette, A. Selmani, Novel injectable neutral solutions of chitosan form biodegradable gels in situ, *Biomaterials* 21 (2000) 2155–2161.
- [34] W.-C. Huang, S.-H. Hu, K.-H. Liu, S.-Y. Chen, D.-M. Liu, A flexible drug delivery chip for the magnetically-controlled release of anti-epileptic drugs, *J. Control. Release* 139 (2009) 221–228.